ON THE CHOICE OF WINDOW FOR SPATIAL SMOOTHING OF SPHERICAL DATA

Zubair Khalid, Rodney A. Kennedy and Salman Durrani

Research School of Engineering, The Australian National University, Canberra, ACT 0200, Australia
Email: {zubair.khalid, rodney.kennedy, salman.durrani}@anu.edu.au

ABSTRACT

This paper investigates spectral filtering using isotropic spectral windows, which is a computationally efficient method of spatial smoothing on the sphere. We propose a Slepian eigenfunction window, which is obtained as a solution of the concentration problem on the sphere, as a good choice of the window function. We also unify a comprehensive set of quantitative tools, both spatial and spectral, to assess and compare the performance of different smoothing windows (i.e., smoothers). We analyze and compare the performance of the proposed window against the two best available candidates in the literature: von-Hann window and von Mises-Fisher distribution window. We establish that the latter window includes the popular Gauss window as a subcase. We show that the Slepian eigenfunction window has the smallest spatial variance (better spatial localization) and the smallest side-lobe level.

Index Terms— 2-sphere; unit sphere; windows; convolution; smoothing; spherical harmonic transform.

1. INTRODUCTION

Signals are naturally defined on the 2-sphere in a variety of science and engineering disciplines including geodesy [1, 2], cosmology [3], biomedical imaging [4], and wireless channel modeling [5]. Smoothing of such signals in the spatial domain, for noise reduction or for band-limiting the signal, is often carried out as isotropic convolution [1–4, 6–8], which corresponds to the windowing of the signal in the spectral domain. The choice of the window function is, therefore, crucial in the smoothing process.

1.1. Relation to Prior Work

Many window functions have been proposed for spatial smoothing of signals on the sphere, either in the spatial or the spectral domain [1–4, 7]. Ideally, the window should be (i) a rectangular shape (sharp cut-off) in the spectral domain such that complete information is preserved while band-limiting the signal and (ii) a Dirac delta in the spatial domain to avoid accumulation of the signal at each spatial position from the neighbouring signal components. However, these ideal characteristics in both the spatial and the spectral domains cannot be achieved simultaneously by virtue of the uncertainty principle. Hence, smoothed or tapered spectral windows are often used in practice. For example, the Gauss window has been used in geodesy for isotropic smoothing of gravity data observed over the sphere [1, 2]. The von Mises-Fisher distribution window has been used to perform isotropic convolution for smoothing cosmological observations [3]. Furthermore, Guass-Weistrass window is used for diffusion-based spatial smoothing over the sphere [7] and for smoothing of cortical surfaces in biomedical imaging [4], where it has been termed as the heat kernel.

Recently, spatial and spectral measures to compare the performance of different spectral windows were proposed in [8] and it was shown that the von-Hann window serves as a good choice for spectral windowing. However [8] analysed the window functions popular in geodesy by adapting the measures of performance in [9] and did not consider some other measures [4, 10] and windows [3, 7].

1.2. Contributions

In this work, we propose to use the suitably selected eigenfunction window for isotropic convolution (spectral windowing). The proposed window is obtained as a solution of Slepian concentration problem on the sphere [11–13]. We also unify the different figures of merit in the literature to measure and analyse the performance of different smoothing windows (i.e., smoothers). We analyse the von-Hann, von Mises-Fisher distribution (Gauss) and eigenfunction windows and show that the proposed eigenfunction window serves as a better choice in terms of a number of spatial and spectral performance measures.

The paper is organized as follows. The mathematical background and window functions are reviewed in Section 2. The problem statement is defined in Section 3. The measures for quantifying the performance of the smoothers are presented in Section 4. The results are discussed in Section 5.

2. PRELIMINARIES

2.1. Signals and Systems on the 2-Sphere

We consider the complex Hilbert space finite energy functions on the 2-sphere, $L^2(\mathbb{S}^2)$, which is equipped with the following inner product

$$\langle f, h\rangle \triangleq \int_{\mathbb{S}^2} f(\widehat{\boldsymbol{x}})\,\overline{h(\widehat{\boldsymbol{x}})}\,ds(\widehat{\boldsymbol{x}}), \tag{1}$$

where $\widehat{\boldsymbol{x}} \equiv \widehat{\boldsymbol{x}}(\theta,\phi) \triangleq (\sin\theta\cos\phi,\ \sin\theta\sin\phi,\ \cos\theta) \in \mathbb{R}^3$ is a unit vector which parameterizes a point on the 2-sphere, $\mathbb{S}^2$, $ds(\widehat{\boldsymbol{x}}) = \sin\theta\, d\theta\, d\phi$ and $\overline{(\cdot)}$ denotes complex conjugate. $\theta \in [0,\pi]$ denotes the co-latitude measured with respect to the positive z-axis and $\phi \in [0, 2\pi)$ denotes the longitude measured with respect to the positive x-axis in the x-y plane. The inner product in (1) induces a norm $\|f\| \triangleq \langle f, f\rangle^{1/2}$, and the functions with finite induced norm are referred as signals on the 2-sphere in this paper.

Spherical harmonics [14] defined for integer degree $\ell \geq 0$ and integer order $m \in [-\ell, \ell]$ form archetype complete orthonormal set of basis functions for $L^2(\mathbb{S}^2)$ and are expressed as follows

$$Y_\ell^m(\theta,\phi) \triangleq \sqrt{\frac{2\ell+1}{4\pi}\frac{(\ell-m)!}{(\ell+m)!}}P_\ell^m(\cos\theta)e^{im\phi} \equiv Y_\ell^m(\widehat{\boldsymbol{x}}),$$

This work was supported under the Australian Research Council's Linkage Projects funding scheme (project no. LP100100588).

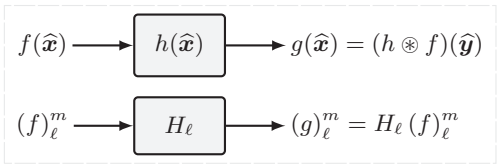

Fig. 1: Isotropic convolution (upper) and spectral smoothing (lower).

where P_ℓ^m denotes the associated Legendre function [14]. By completeness of spherical harmonics, we can expand any signal $f \in L^2(\mathbb{S}^2)$ as

$$f(\widehat{\boldsymbol{x}}) = \sum_{\ell=0}^{\infty} \sum_{m=-\ell}^{\ell} (f)_\ell^m Y_\ell^m(\widehat{\boldsymbol{x}}), \quad (f)_\ell^m \triangleq \langle f, Y_\ell^m \rangle, \tag{2}$$

where $(f)_\ell^m$ denotes the spherical harmonic Fourier coefficient of degree ℓ and order m. The signal f is said to be *band-limited at degree* L if $(f)_\ell^m = 0$, $\forall \ell > L$.

A signal $h(\widehat{\boldsymbol{x}})$ is said to be azimuthally symmetric when $h(\widehat{\boldsymbol{x}}) = h(\theta, \phi) = h(\theta)$). The set of azimuthally symmetric functions of the form $h(\widehat{\boldsymbol{x}}) = h(\theta, \phi) = h(\theta)$ forms a subspace of $L^2(\mathbb{S}^2)$ and is denoted by $\mathcal{H}^0$. Define the rotation operator $\mathcal{D}(\widehat{\boldsymbol{y}})$ with $\widehat{\boldsymbol{y}} = \widehat{\boldsymbol{y}}(\vartheta, \varphi)$ that rotates an azimuthally symmetric function $h(\widehat{\boldsymbol{x}}) \in \mathcal{H}^0$ by $\vartheta \in [0,\, \pi]$ about y-axis followed by $\varphi \in [0,\, 2\pi)$ about z-axis. Then [14]

$$\big(\mathcal{D}(\widehat{\boldsymbol{y}})h\big)_\ell^m = \sqrt{\frac{4\pi}{2\ell+1}}\overline{Y_\ell^m(\vartheta,\varphi)}(h)_\ell^0, \quad \widehat{\boldsymbol{y}} = \widehat{\boldsymbol{y}}(\vartheta,\varphi). \tag{3}$$

By the spherical harmonic addition theorem [15], the spatial form is

$$\begin{aligned}\big(\mathcal{D}(\widehat{\boldsymbol{y}})h\big)(\widehat{\boldsymbol{x}}) &= \sum_{\ell=0}^{\infty}\sum_{m=-\ell}^{\ell}\sqrt{\frac{4\pi}{2\ell+1}}(h)_\ell^0\overline{Y_\ell^m(\widehat{\boldsymbol{x}})}Y_\ell^m(\widehat{\boldsymbol{y}}) \\ &= \sum_{\ell=0}^{\infty}(h)_\ell^0\sqrt{\frac{2\ell+1}{4\pi}}P_\ell^0(\widehat{\boldsymbol{x}}\cdot\widehat{\boldsymbol{y}}) = h(\arccos\widehat{\boldsymbol{x}}\cdot\widehat{\boldsymbol{y}}).\end{aligned} \tag{4}$$

2.2. Isotropic Convolution or Spectral Smoothing

Of the many notions of convolution on the sphere [14, 16] we consider isotropic convolution [3, 7, 17, 18], which is also referred to as "spectral smoothing" [4, 7, 8]. Define the convolution between $f \in L^2(\mathbb{S}^2)$ and an azimuthally symmetric $h \in \mathcal{H}^0$ as follows:

$$g(\widehat{\boldsymbol{y}}) \triangleq (h \circledast f)(\widehat{\boldsymbol{y}}) \triangleq \int_{\mathbb{S}^2} f(\widehat{\boldsymbol{x}})\big(\mathcal{D}(\widehat{\boldsymbol{y}})h\big)(\widehat{\boldsymbol{x}})ds(\widehat{\boldsymbol{x}}), \tag{5}$$

and in spectral form, depicted in Fig. 1,

$$(g)_\ell^m = \underbrace{\sqrt{\frac{4\pi}{2\ell+1}}(h)_\ell^0}_{\triangleq\, H_\ell}(f)_\ell^m, \tag{6}$$

which makes it evident that "spectral smoothing" is taking place, at least when the H_ℓ are all positive. The H_ℓ characterize the spectral window and we present a number of examples next.

2.3. Basic Smoothers and Spectral Windows

In the literature either the spatial form, (5), or the spectral form, (6), of a smoothing operator is given in closed-form as revealed in our following list. (A closed-form spatial form may not have a closed-form spectral form and vice versa.)

Rectangular Window (Spectral): This window performs spectral truncation up to an including band-limit parameter L:

$$H_\ell(L) = \begin{cases} 1 & \ell \in \{0, 1, \ldots, L\} \\ 0 & \text{otherwise,} \end{cases} \tag{7}$$

which has unit energy normalization

Gauss Window (Spatial): Gauss window has been used for smoothing gravity models in geophysics [1, 2] and is defined as follows:

$$h(\theta; \theta_{\text{FWHM}}) = b\,\frac{e^{-b(1-\cos\theta_c)}}{1-e^{-2b}}, \quad b = \frac{\ln 2}{1-\cos\theta_{\text{FWHM}}} \tag{8}$$

where the parameter $\theta_{\text{FWHM}} > 0$ indicates the degree of smoothness.

von-Hann Window (Spatial): The von-Hann window, commonly know as Hanning window or raised cosine window in Euclidean domain [9], is defined in terms of the width of the main lobe θ_c as follows:

$$h(\theta; \theta_c) = \begin{cases} \frac{1}{2}\big(1 + \cos(\pi\theta/\theta_c)\big) & 0 \le \theta \le \theta_c \\ 0 & \text{otherwise.} \end{cases} \tag{9}$$

von Mises-Fisher Distribution Window (Spatial and Spectral): The von Mises-Fisher distribution window (or von Mises-Fisher window) has been used in literature for isotropic smoothing in cosmology [3] and is defined for the concentration parameter $\kappa \ge 0$ with known spectral domain representation [19]

$$h(\theta; \kappa) \triangleq \frac{\kappa\exp(\kappa\,\cos\theta)}{4\pi\sinh\kappa}, \quad H_\ell(\kappa) = \frac{I_{\ell+1/2}(\kappa)}{I_{1/2}(\kappa)}, \tag{10}$$

where $I_{\ell+1/2}(\cdot)$ denotes half-integer-order modified Bessel function of the first kind. We observe that, in fact, the von Mises-Fisher distribution window and the Gauss window are identical when $\kappa = b$.

Gauss-Weierstrass Window (Spectral): This window has the following spectral characterization for $\kappa \ge 0$

$$H_\ell(\kappa) = e^{-\ell(\ell+1)/(2\kappa)} \tag{11}$$

has been used for spherical diffusion [7] and also for spectral smoothing of cortical surfaces [4]. We note that the Gauss-Weierstrass window is an asymptotic form of the von Mises-Fisher distribution window for large values of the parameter κ [3].

2.4. Slepian Eigenfunction Window

With two parameters, the band-limit L and angular size θ_c, one can solve a Slepian concentration problem on the sphere, which finds the band-limited function that maximizes the proportion of energy that falls within the polar cap region $\theta \in [0, \theta_c]$, see [11–13]. This function is the eigenfunction with the largest eigenvalue of an associated integral equation. Generally the concentration is high (close to unity) unless both L and θ_c are simultaneously too small. The specific "Slepian eigenfunction window" we refer to in this section is one where both L and θ_c are simultaneous as small as possible in the following sense:

$$\theta_c = \frac{2\pi}{L+1}. \tag{12}$$

for which it can be established that one eigenfunction is at least 99% concentrated [12, 20]. Therefore, using (12) we have a one parameter "eigenfunction window" family parametrized (without loss of generality) by L.

The eigenfunction window $h \in \mathcal{H}^0$ with band-limit L and energy concentration within cap angle θ_c, given in (12), can be computed in spectral domain as a solution of following algebraic eigenvalue problem [12, 20]

$$\mathbf{D}\mathbf{h} = \lambda\mathbf{h}, \tag{13}$$

where $\mathbf{h} = [(h)_0^0, (h)_1^0, \ldots, (h)_L^0]$ and $\mathbf{D}$ is the $(L+1)\times(L+1)$ real and symmetric matrix with entries given by

$$D_{\ell,\ell'} = 2\pi\int_0^{\theta_c} Y_\ell^0(\theta,0)Y_{\ell'}^0(\theta,0)\sin\theta\,d\theta, \tag{14}$$

which can be computed analytically [12], however, requires the computation of Wigner-3j symbols [21]. Alternatively, the eigenvalue problem in (13) can be solved as an eigen decomposition of the matrix $\mathbf{G}$ of size $(L+1)\times(L+1)$ that commutes with $\mathbf{D}$, that is, $\mathbf{DG}=\mathbf{GD}$. It has been shown that $\mathbf{G}$ is a tridiagonal matrix with entries of the form [13]

$$G_{\ell,\ell+1}=G_{\ell+1,\ell}=\frac{(\ell+1)\left(\ell(\ell+2)-(L)(L+2)\right)}{\sqrt{(2\ell+1)(2\ell+3)}},$$
$$G_{\ell,\ell}=-\ell(\ell+1)\cos(\theta_c),\quad G_{\ell,\ell'}=0. \tag{15}$$

Since $\mathbf{G}$ is a tridiagonal matrix with simple entries given in (15), its eigen decomposition can be easily obtained and gives $L+1$ eigenvectors of the form $\mathbf{h}$ and the one with the *smallest* eigenvalue yields the spectral domain representation of the desired eigenfunction window. This procedure furnishes $(h)_\ell^0$ which are readily scaled to give the H_ℓ shown in (6) and Fig. 1. Neither the spatial form, (5), nor the spectral form, (6), of a smoothing operator are closed-form but can be easily obtained by the eigen decomposition of $\mathbf{G}$.

3. PROBLEM STATEMENT

Isotropic convolution or spectral smoothing are used to reduce the effects of noise [2], to perform basic low-pass filtering such as forming a band-limited representation of signal and to perform spatial smoothing. For example, rectangular window (7) can be used to band-limit a signal at degree L. However, the choice of such a rectangular window produces ringing artifacts (due to the Gibb's phenomenon [22]) in the spatial domain as noted in [4]. This highlights the need to find objective measure to assess performance and compare different designs for smoothers.

In summary our problem addresses the following issues:

1. to use and develop quantitative tools [8] to quantify smoother performance on the 2-sphere;
2. to implement and assess the performance of the eigenfunction window as a smoother; and
3. to compare the eigenfunction window with smoothers from the literature, [1–4, 7, 8], and Section 2.3.

4. MEASURE FOR QUANTIFYING PERFORMANCE

We categorize measures for quantifying performance into spectral and spatial measures depending on the domain under study. In the derivation of these measures, we assume that the window function under analysis unit energy normalized, that is,

$$2\pi\int_0^\pi \left|h(\theta)\right|^2\sin\theta\,d\theta=1\Longleftrightarrow\sum_{\ell=0}^{\infty}\left|h_\ell\right|^2=\sum_{\ell=0}^{\infty}\frac{2\ell+1}{4\pi}\left|H_\ell\right|^2=1.$$

4.1. Spectral Measures

Spectral Variance: Spectral variance quantifies the spread of the spectral window in the spectral domain. Mathematically, the variance of the window function $h\in\mathcal{H}^0$ in the spectral (Fourier) domain, denoted by σ_F, is defined as [10]

$$\sigma_F^2=4\pi\sum_{\ell=0}^{L}\frac{\ell(\ell+1)}{2\ell+1}\left|H_\ell\right|^2. \tag{16}$$

Since the windowing is applied in spectral domain, a superior window should have large spectral variance for a given band-limit L of the window function.

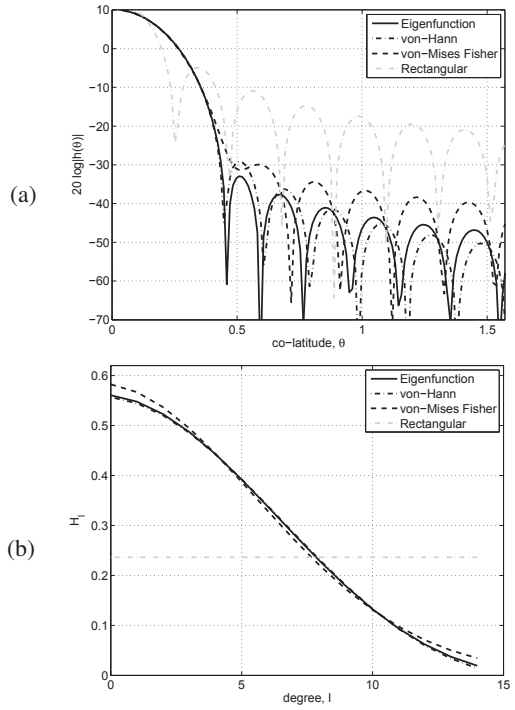

Fig. 2: von Mises-Fisher, von-Hann, rectangular and the eigenfunction windows are plotted in spatial and spectral domains as (a) $h(\theta)$ and (b) H_ℓ respectively. The band-limit for each window is $L=14$ and the common spectral variance is $\sigma_F=36.0980$.

Processing Loss: Due to the smoothness imposed by the spectral window, there is information loss in the spectral domain. We quantify such processing loss for a window with band-limit L as [9]

$$\beta=\big(\sum_{\ell=0}^{L}H_\ell\big)^2. \tag{17}$$

The higher the value of β for a given window, the lower the processing loss due to smoothness of the spectral window.

4.2. Spatial Measures

Since the spectral windowing of the signal with H_ℓ is a consequence of convolution of the signal with a signal $h(\widehat{\boldsymbol{x}})$, we identify the major characteristics of the window function in the spatial domain that will allow us to compare the performance of different windows.

Spatial Variance: The spatial variance serves as a measure of spatial localization or peakiness of the window function around its center (usually taken as the north pole). Mathematically define spatial variance σ_{S}^2 as [10, 20]

$$\sigma_{\mathrm{S}}^2=1-\Big(\pi\int_0^\pi\sin(2\theta)\left|h(\theta)\right|^2d\theta\Big)^2. \tag{18}$$

The smaller value of spatial variance indicates more localization of the window function in the spatial domain, which implies the better performance as this minimizes the accumulation of different signal components.

Full-Width at the Half-Maximum (FWHM): Let FWHM be denoted by θ_{FWHM} and defined as the width from the center (usually $\theta=0$) where the function $h(\widehat{\boldsymbol{x}})$ attains the maximum value, that is,

$$h(\theta_{\mathrm{FWHM}})=\frac{1}{2}h(0)$$

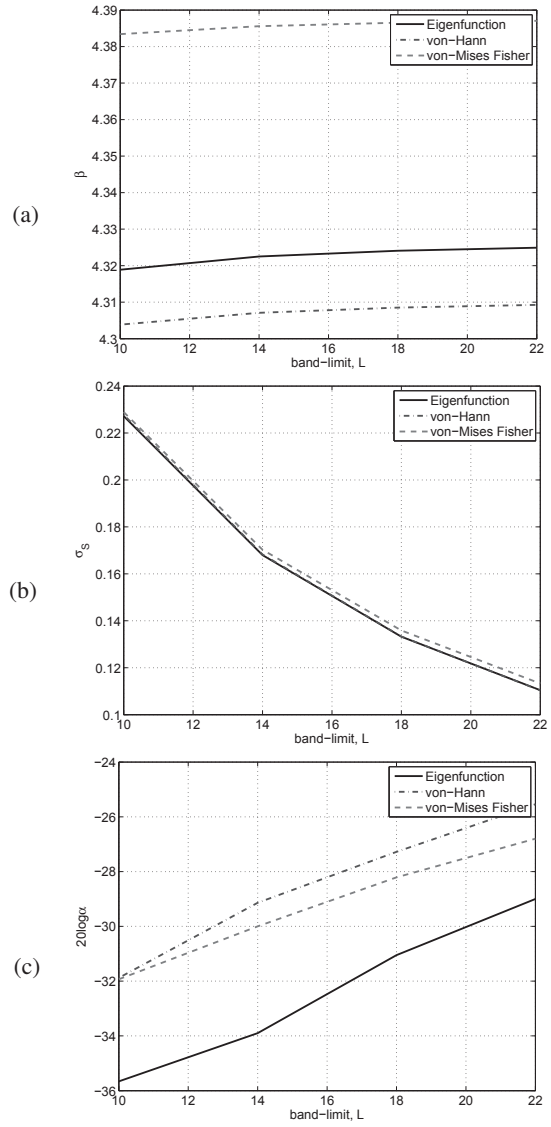

Fig. 3: (a) Processing loss β, (b) spatial variance σ_S, (c) side-lobe level α for windows with band-limits in the range $10 \leq L \leq 22$.

It is a measure of localization of window function and is sometimes referred as 3dB width of the window function [4]. If the separation between the two same strength signal components in the spatial domain is less than twice of FWHM, the two components appear as a single component and will not be resolved in the smoothed signal.

Main-Lobe Energy and Energy Leakage: Main-lobe energy, denoted by $\mathcal{E}_m$, and energy leakage, denoted by $\mathcal{E}_s$, are defined as the energy in the main lobe parameterized by θ_c and the energy outside the main lobe respectively, that is,

$$\mathcal{E}_m = 2\pi \int_0^{\theta_c} \left|h(\theta)\right|^2 \sin\theta \, d\theta, \quad \mathcal{E}_s = 1 - \mathcal{E}_m. \tag{19}$$

The larger value of $\mathcal{E}_m$ indicates better performance.

Side-lobe Level: Side-lobe level is defined as the magnitude of the highest side-lobe. This is an important measure as it quantifies the accumulation of the largest unwanted contribution outside the main-lobe. We use α to denote the magnitude of the highest side-lobe.

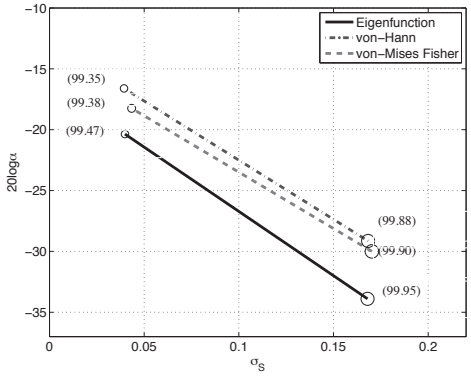

Fig. 4: The trade-off (quantified by the slope) between spatial variance σ_S and side-lobe level α. The right and left markers denote the windows with $L = 14$ and $L = 64$, respectively. The radius of marker is proportional to the width of the main-lobe and the value in brackets indicates the main-lobe energy concentration $\mathcal{E}_m$.

5. PERFORMANCE COMPARISON

Fair Comparison Strategy: Here we use the measures defined in Section 4 to compare the performance of the von Mises-Fisher, von-Hann, rectangular and the eigenfunction windows (as the von Mises-Fisher distribution and Gauss window are equivalent and the Gauss-Weierstrass asymptotically equivalent). Since the windows are defined by different parameters, we devise the following strategy in order to carry out meaningful comparison: 1) for given L, determine θ_c using (12) and determine the eigenfunction window; and 2) choose parameters of von Mises-Fisher distribution window and von-Hann window such that each window function, when band-limited at L, is unit energy normalized and has the spectral variance σ_F equal to that of eigenfunction window.

Analysis Results: For $L = 14$, the different windows are plotted in Fig. 2(a) and (b) in spatial domain as $h(\theta)$ and spectral domain as H_ℓ respectively. It is evident that the eigenfunction window has better spatial localization and smaller side-lobe level.

We compare the processing loss (β), spatial variance (σ_S) and side-lobe level (α) for windows with band-limits in the range $10 \leq L \leq 22$ in Fig. 3(a), (b) and (c) respectively. von Mises-Fisher distribution window has the higher (better) processing loss. However, the processing loss does not vary with the band-limit. The eigenfunction window has the smallest spatial variance (better spatial localization) and the smallest side-lobe level.

In order to further study the trade-off between spatial variance and side-lobe level, we plot the spatial variance versus side-lobe level in Fig. 4 for different windows, where it can be observed that eigenfunction window has better performance as compared to the von-Hann window and von Mises-Fisher distribution window.

6. CONCLUSIONS

In this work, we have categorised the different figures of merit to compare the performance of different spectral windows for spatial smoothing. Based on the comparison with other windows: von-Hann and von Mises-Fisher (Gauss), we have proposed the use of eigenfunction window, obtained as a solution of Slepian concentration problem on the sphere. We have shown that the eigenfunction window is more localized in spatial domain and also exhibits the smaller side-lobe level and therefore reduces the accumulation of different signal components in the spatial domain.

7. REFERENCES

[1] C. Jekeli, "Alternative methods to smooth the Earth's gravity field," Dep. of Geod. Sci. and Surv., Ohio State Univ., Columbus, Tech. Rep. Rep. 327, 1981.

[2] J. Wahr, M. Molenaar, and F. Bryan, "Time variability of the Earth's gravity field: Hydrological and oceanic effects and their possible detection using GRACE," *J. Geophys. Res.*, vol. 103, no. B12, pp. 30 205–30 229, Dec. 1998.

[3] K.-I. Seon, "Smoothing of all-sky survey map with Fisher-von Mises function," *J. Korean Phys. Soc.*, vol. 48, no. 3, pp. 331–334, Mar. 2006.

[4] M. K. Chung, K. M. Dalton, L. Shen, A. C. Evans, and R. J. Davidson, "Weighted Fourier series representation and its application to quantifying the amount of gray matter," *IEEE Trans. Med. Imag.*, vol. 26, no. 4, pp. 566–581, Apr. 2007.

[5] T. S. Pollock, T. D. Abhayapala, and R. A. Kennedy, "Introducing space into MIMO capacity calculations," *J. Telecommun. Syst.*, vol. 24, no. 2, pp. 415–436, Oct. 2003.

[6] J. R. Driscoll and D. M. Healy, Jr., "Computing Fourier transforms and convolutions on the 2-sphere," *Adv. Appl. Math.*, vol. 15, no. 2, pp. 202–250, Jun. 1994.

[7] T. Bülow, "Spherical diffusion for 3D surface smoothing," *IEEE Trans. Pattern Anal. Mach. Intell.*, vol. 26, no. 12, pp. 1650–1654, Dec. 2004.

[8] B. Devaraju and N. Sneeuw, "Performance analysis of isotropic spherical harmonic spectral windows," in *VII Hotine-Marussi Symposium on Mathematical Geodesy*, ser. International Association of Geodesy Symposia. Springer Berlin Heidelberg, 2012, vol. 137, pp. 105–110.

[9] F. J. Harris, "On the use of windows for harmonic analysis with the discrete Fourier transform," *Proc. IEEE*, vol. 66, no. 1, pp. 51–83, Jan. 1978.

[10] F. J. Narcowich and J. D. Ward, "Nonstationary wavelets on the m-sphere for scattered data," *Appl. Comput. Harmon. Anal.*, vol. 3, no. 4, pp. 324–336, Oct. 1996.

[11] A. Albertella, F. Sansò, and N. Sneeuw, "Band-limited functions on a bounded spherical domain: the Slepian problem on the sphere," *J. Geodesy*, vol. 73, no. 9, pp. 436–447, Jun. 1999.

[12] M. A. Wieczorek and F. J. Simons, "Localized spectral analysis on the sphere," *Geophys. J. Int.*, vol. 162, no. 3, pp. 655–675, May 2005.

[13] F. J. Simons, F. A. Dahlen, and M. A. Wieczorek, "Spatiospectral concentration on a sphere," *SIAM Rev.*, vol. 48, no. 3, pp. 504–536, 2006.

[14] R. A. Kennedy and P. Sadeghi, *Hilbert Space Methods in Signal Processing*. Cambridge, UK: Cambridge University Press, Mar. 2013.

[15] D. Colton and R. Kress, *Inverse Acoustic and Electromagnetic Scattering Theory*, 2nd ed. Berlin: Springer-Verlag, 1998.

[16] P. Sadeghi, R. A. Kennedy, and Z. Khalid, "Commutative anisotropic convolution on the 2-sphere," *IEEE Trans. Signal Process.*, vol. 60, no. 12, pp. 6697–6703, Dec. 2012.

[17] M. Tegmark, D. H. Hartmann, M. S. Briggs, and C. A. Meegan, "The angular power spectrum of BATSE 3B gamma-ray bursts," *Astrophys. J.*, vol. 468, pp. 214–224, Sep. 1996.

[18] R. A. Kennedy, T. A. Lamahewa, and L. Wei, "On azimuthally symmetric 2-sphere convolution," *Digital Signal Process.*, vol. 5, no. 11, pp. 660–666, Sep. 2011.

[19] K. Mammasis and R. W. Stewart, "Spherical statistics and spatial correlation for multielement antenna systems," *EURASIP J. Wirel. Commun.*, vol. 2010, Dec. 2010, article ID 307265.

[20] Z. Khalid, S. Durrani, P. Sadeghi, and R. A. Kennedy, "Spatio-spectral analysis on the sphere using spatially localized spherical harmonics transform," *IEEE Trans. Signal Process.*, vol. 60, no. 3, pp. 1487–1492, Mar. 2012.

[21] J. J. Sakurai, *Modern Quantum Mechanics*. Reading, MA: Addison-Wesley Publishing Company, Inc., 1994.

[22] A. Gelb, "The resolution of the Gibbs phenomenon for spherical harmonics," *Math. Comp.*, vol. 66, no. 218, pp. 699–717, Apr. 1997.